Numerical Evaluation of Dyadic Diffraction Coefficients and Bistatic Radar Cross Sections for a Perfectly Conducting Semi-Infinite Elliptic Cone

Siegfried Blume and Volker Krebs

***Abstract*—In this paper, the scattering of electromagnetic waves by a perfectly conducting semi-infinite elliptic cone is treated. The exact solution of this boundary value problem in problem-adapted spheroconal coordinates in the form of a spherical multipole expansion is of poor convergence if both the source point and the field point are far away from the cone's tip. Therefore, an appropriate sequence transformation of these series expansions (we apply the Shanks transformation) is necessary to numerically determine the dyadic diffraction coefficients and bistatic radar cross sections (RCS) for an arbitrary elliptic cone. Our far-field data for an elliptic cone, a circular cone, and a plane angular sector are compared with some other results obtained with the aid of quite different methods.**

***Index Terms*—Electromagnetic diffraction, radar cross section.**

I. Introduction

RECENTLY, an article dealing with electromagnetic scattering by a perfectly conducting semi-infinite cone of arbitrary shape was published by Babich *et al*. [1]. The solution was synthesized via the superposition of the solutions of the two associated scalar problems—the acoustical scattering by a soft or hard cone. The treatment of the boundary value problems leads to integral equations of the Fredholm type along the line of intersection of the cone and the unit sphere. Numerical evaluations of bistatic radar cross sections (RCS) were performed for a semi-infinite perfectly conducting circular cone and an elliptic cone.

Appropriate uniform solutions that make the asymptotic high-frequency total field continuous across the shadow boundaries of the rays diffracted by a circular cone or by a plane angular sector (two degenerations of an elliptic cone) were derived in [2]–[4].

Hill's uniform solution for the plane angular sector is based upon the solutions of the two associated scalar problems. Trott's uniform solution for the circular cone was obtained from the evaluation of the radiating integral for the scattered field using a geometrical optics (GO) approximation for the surface current on the cone and an exact kernel rather than the far-zone form for the scalar Green's function. Assuming the observation point is on the shadow side of the reflection shadow boundary his solution yields the same result as that obtained via the exact evaluation of the physical optics (PO) far-zone fields of the circular cone and is simply the nonuniform asymptotic result for the tip diffracted contribution. These PO-based far-zone fields of a circular cone will be compared with the far-zone fields of the rigorous multipole solution to be developed.

A PO approximation of the bistatic RCS of an elliptic cone was derived in [5]. In the case of a circular cone, this formula coincides with the PO-based solution derived by Trott.

The interest in these problems is motivated by the role in which the diffraction coefficients play in asymptotic high-frequency theories like the geometrical theory of diffraction (GTD) or the uniform theory of diffraction (UTD). These ray-optical techniques represent extensions of classical GO by introducing diffracted rays produced when incident rays hit edges, corners, tips, or impinge tangentially on smoothly curved surfaces of scattering objects. The initial value of the field on a diffracted ray is, according to the principle of locality in the GTD or UTD, determined from the incident field at the point of diffraction with the aid of an appropriate diffraction coefficient. These diffraction coefficients are to be determined from the solution of boundary value problems with simple shapes (canonical structures) capable of approaching the local geometry at the point of diffraction. One of the incompletely solved canonical problems in the electromagnetic theory is that of diffraction by a semi-infinite elliptic cone. The rigorous treatment of scattering by this structure and the numerical evaluation of diffraction coefficients and bistatic RCS are the subjects of this paper. A comprehensive review, dedicated to the solution of this boundary value problem, is to be found in [6]–[8]. Pioneering work has been carried out by Kraus and Levine, who examined scalar diffraction by a semi-infinite elliptic cone with the aid of the same technique [9].

The paper proceeds as follows. In Section II, the spheroconal or conical coordinate system is introduced. Appropriate elementary solutions of the scalar Helmholtz equation and the spherical multipole expansion of the electromagnetic field in these problem-adapted conical coordinates will be presented in Section III. The scattering of electromagnetic waves by a perfectly conducting semi-infinite elliptic cone and the introduction of dyadic diffraction coefficients and of bistatic RCS will be treated in Section IV. In order to improve the rapidity of convergence of the rigorous modal series expansions and to obtain numerical results, the nonlinear Shanks transformation is introduced in Section V. In Section VI, we compare our far-field data for a circular cone, for an elliptic cone, and for

Manuscript received October 7, 1996; revised November 18, 1997.

The authors are with the Department of Electrical Engineering, Ruhr-Universität Bochum, Bochum, D-44780 Germany.

Publisher Item Identifier S 0018-926X(98)02272-8.

a plane angular sector with the published data in the papers [1]–[5].

Throughout the paper, a time dependence of $e^{+j\omega t}$ will be assumed but always suppressed.

II. Spheroconal Coordinates

We introduce a spheroconal coordinate system (r, ϑ, φ) related to the cartesian coordinate system by the transformation

$$x = r\sin\vartheta\cos\varphi, \qquad 0 \le r < \infty \tag{1}$$

$$y = r\sqrt{1 - k^2\cos^2\vartheta}\sin\varphi, \qquad 0 \le \vartheta \le \pi \tag{2}$$

$$z = r\cos\vartheta\sqrt{1 - k'^2\sin^2\varphi}, \qquad 0 \le \varphi \le 2\pi. \tag{3}$$

k and k' are ellipticity parameters with

$$0 \le k, k' \le 1; \qquad k^2 + k'^2 = 1. \tag{4}$$

In the special case $k = 1$ $(k' = 0)$ the spheroconal coordinate system (r, ϑ, φ) reduces to the ordinary spherical coordinate system denoted by $(r, \overline{\vartheta}, \overline{\varphi})$.

The coordinate surfaces are (Fig. 1):

- $r = r_c$ spherical surfaces around the origin;
- $\vartheta = \vartheta_c$ semi-infinite elliptic cones around the z axis with their cone tips in the origin, with half-opening angles α_x in the xz plane, and α_y in the yz plane;
- $\varphi = \varphi_c$ one half of semi-infinite elliptic cones around the y axis.

It can be shown that there are the following relationships between $\vartheta_c, \alpha_x, \alpha_y$ and k:

$$\alpha_x = \pi - \vartheta_c, \quad \alpha_y = \pi - \arccos(k\cos\vartheta_c), \quad k = \frac{\cos\alpha_y}{\cos\alpha_x}.$$

III. Multipole Expansion of the Electromagnetic Field

The key to the solution of the scattering problem is the knowledge of the elementary solutions of Maxwell's equations in a source-free region in the conical coordinate system. In a source-free region the electric $(\vec{E})$ and magnetic $(\vec{H})$ field intensities are solutions of the homogeneous vector differential equations

$$\vec{\nabla}\times\vec{\nabla}\times\vec{E} - \kappa^2\vec{E} = 0, \quad \vec{\nabla}\times\vec{\nabla}\times\vec{H} - \kappa^2\vec{H} = 0 \tag{5}$$

where $\kappa = \omega\sqrt{\epsilon\mu} = 2\pi/\Lambda$ is the wavenumber and Λ the wavelength. Linear independent solenoidal solutions are the vector spherical-multipole functions (Stratton [10])

$$\vec{M}_\nu = (\vec{r}\times\vec{\nabla})\Psi_\nu \quad \vec{N}_\nu = \frac{1}{\kappa}[\vec{\nabla}\times(\vec{r}\times\vec{\nabla})]\Psi_\nu \tag{6}$$

where Ψ_ν is a solution of the scalar homogeneous Helmholtz equation

$$\vec{\nabla}^2\Psi_\nu + \kappa^2\Psi_\nu = 0. \tag{7}$$

In conical coordinates the elementary solutions Ψ_ν can be written in the separated form

$$\Psi_\nu = z_\nu(\kappa r)Y_\nu(\vartheta, \varphi). \tag{8}$$

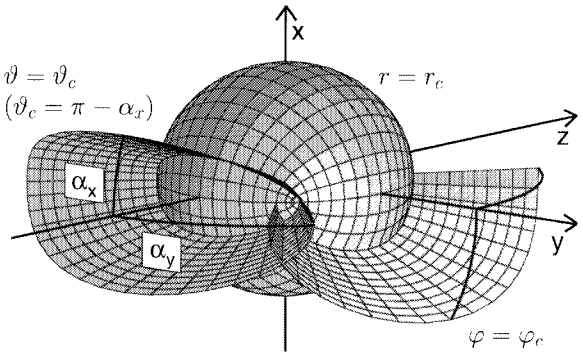

Fig. 1. Spheroconal coordinate surfaces.

The spherical cylinder functions $z_\nu(\kappa r)$ are related to cylinder functions of order $\nu + \frac{1}{2}$ according to

$$z_\nu(\kappa r) = \sqrt{\frac{\pi}{2\kappa r}}Z_{\nu+(1/2)}(\kappa r). \tag{9}$$

Spherical Bessel functions are denoted by $j_\nu(\kappa r)$; spherical Hankel functions of the second kind are denoted by $h_\nu^{(2)}(\kappa r)$. The spherical harmonics $Y_\nu(\vartheta, \varphi)$ satisfying the eigenvalue equation

$$(\vec{r}\times\vec{\nabla})^2 Y_\nu(\vartheta, \varphi) = -\nu(\nu+1)Y_\nu(\vartheta, \varphi) \tag{10}$$

may be written as "Lamé products"

$$Y_\nu^{(p)}(\vartheta, \varphi) = \Theta_\nu^{(p)}(\vartheta)\Phi_\nu^{(p)}(\varphi), \qquad p = 1; 2; 3; 4. \tag{11}$$

The upper index p indicates the existence of four function types. The periodic Lamé functions $\Phi_\nu^{(p)}(\varphi)$ and nonperiodic Lamé functions $\Theta_\nu^{(p)}(\vartheta)$ are solutions of the two coupled Lamé differential equations with separation constants (λ, ν)

$$\sqrt{1 - k'^2\sin^2\varphi}\frac{d}{d\varphi}\left(\sqrt{1 - k'^2\sin^2\varphi}\frac{d\Phi_\nu^{(p)}(\varphi)}{d\varphi}\right) + [\lambda - \nu(\nu+1)k'^2\sin^2\varphi]\Phi_\nu^{(p)}(\varphi) = 0 \tag{12}$$

$$\sqrt{1 - k^2\cos^2\vartheta}\frac{d}{d\vartheta}\left(\sqrt{1 - k^2\cos^2\vartheta}\frac{d\Theta_\nu^{(p)}(\vartheta)}{d\vartheta}\right) + [\nu(\nu+1)(1 - k^2\cos^2\vartheta) - \lambda]\Theta_\nu^{(p)}(\vartheta) = 0. \tag{13}$$

The four types of periodic Lamé functions with the symmetry relations indicated in Table I may be written as Fourier series with periods of π or 2π, where A_{2i}, A_{2i+1}, B_{2i+2}, B_{2i+1} are the Fourier coefficients which have to be determined by three-term recurrence relations leading to tridiagonal matrices.

The four types of nonperiodic Lamé functions can be written as series with associated Legendre functions $P_\nu^m(\cos\vartheta)$ with the same Fourier coefficients. A more detailed analysis is to be found in [11] and [12].

Additionally, the Lamé products are normalized according to

$$\int_0^{\vartheta_c}\int_0^{2\pi}[Y_\nu(\vartheta, \varphi)]^2 s_\vartheta\, s_\varphi\, d\vartheta\, d\varphi = 1 \tag{14}$$

TABLE I
PERIODIC AND NONPERIODIC LAMÉ FUNCTIONS

Periodic Lamé functions		Period		$\varphi = 0$		$\varphi = \pi/2$	
p	Representation	π	2π	even	odd	even	odd
1	$\Phi_\nu^{(1)}(\varphi) = \sum_{i=0}^{\infty} A_{2i} \cos 2i\varphi$	•		•		•	
2	$\Phi_\nu^{(2)}(\varphi) = \sum_{i=0}^{\infty} A_{2i+1} \cos(2i+1)\varphi$		•	•			•
3	$\Phi_\nu^{(3)}(\varphi) = \sum_{i=0}^{\infty} B_{2i+2} \sin(2i+2)\varphi$	•			•		•
4	$\Phi_\nu^{(4)}(\varphi) = \sum_{i=0}^{\infty} B_{2i+1} \sin(2i+1)\varphi$		•		•	•	

Non-periodic Lamé functions		$\vartheta = 0$	
p	Representation	even	odd
1	$\Theta_\nu^{(1)}(\vartheta) = \sum_{i=0}^{\infty} T(2i) A_{2i} P_\nu^{2i}(\cos\vartheta)$	•	
2	$\Theta_\nu^{(2)}(\vartheta) = \sum_{i=0}^{\infty} T(2i+1) A_{2i+1} P_\nu^{2i+1}(\cos\vartheta)$		•
3	$\Theta_\nu^{(3)}(\vartheta) = f(\vartheta) \sum_{i=0}^{\infty} (2i+2) T(2i+2) B_{2i+2} P_\nu^{2i+2}(\cos\vartheta)$		•
4	$\Theta_\nu^{(4)}(\vartheta) = f(\vartheta) \sum_{i=0}^{\infty} (2i+1) T(2i+1) B_{2i+1} P_\nu^{2i+1}(\cos\vartheta)$	•	

$$T(i) = -(\nu - i)(\nu + i + 1)T(i+2) \qquad T(0) = T(1) = 1$$

$$f(\vartheta) = \sqrt{1 - k^2 \cos^2\vartheta}/\sin\vartheta$$

where s_ϑ and s_φ are normalized metric coefficients

$$s_\vartheta = \sqrt{\frac{k^2 \sin^2\vartheta + k'^2 \cos^2\varphi}{1 - k^2\cos^2\vartheta}}$$

$$s_\varphi = \sqrt{\frac{k^2 \sin^2\vartheta + k'^2 \cos^2\varphi}{1 - k'^2\sin^2\vartheta}}. \tag{15}$$

With (6) and (8) the vector-spherical multipole functions can now be expressed in terms of angular vector functions $\vec{m}_\nu$ and $\vec{n}_\nu$

$$\vec{M}_\nu(\vec{r}) = z_\nu(\kappa r)\vec{m}_\nu(\vartheta,\varphi) \tag{16}$$

$$\vec{N}_\nu(\vec{r}) = -\nu(\nu+1)\frac{z_\nu(\kappa r)}{\kappa r} Y_\nu(\vartheta,\varphi)\hat{r} - \frac{1}{\kappa r}\frac{d}{dr}[r z_\nu(\kappa r)]\vec{n}_\nu(\vartheta,\varphi) \tag{17}$$

where

$$\vec{m}_\nu(\vartheta,\varphi) = -\frac{1}{s_\varphi}\frac{\partial Y_\nu(\vartheta,\varphi)}{\partial\varphi}\hat{\vartheta} + \frac{1}{s_\vartheta}\frac{\partial Y_\nu(\vartheta,\varphi)}{\partial\vartheta}\hat{\varphi} \tag{18}$$

$$\vec{n}_\nu(\vartheta,\varphi) = \frac{1}{s_\vartheta}\frac{\partial Y_\nu(\vartheta,\varphi)}{\partial\vartheta}\hat{\vartheta} + \frac{1}{s_\varphi}\frac{\partial Y_\nu(\vartheta,\varphi)}{\partial\varphi}\hat{\varphi}. \tag{19}$$

At the cone's surface, the electric field intensity must satisfy the boundary condition

$$(\vec{n} \times \vec{E})|_{\vartheta=\vartheta_c} = 0 \tag{20}$$

which leads to the transcendental eigenvalue equations for the associated scalar problems

$$\Theta_\sigma^{(p)}(\vartheta)|_{\vartheta=\vartheta_c} = 0 \quad \text{(soft cone: corresponding eigenvalues } \cdot\ \nu \text{ are denoted by } \sigma) \tag{21}$$

$$\left.\frac{d\Theta_\tau^{(p)}(\vartheta)}{d\vartheta}\right|_{\vartheta=\vartheta_c} = 0 \quad \text{(hard cone: corresponding } \cdot \text{ eigenvalues } \nu \text{ are denoted by } \tau). \tag{22}$$

These transcendental equations must be solved numerically. The spherical multipole representation of the electromagnetic field is a superposition of TM and TE modes

$$\vec{E}(\vec{r}) = \sum_\sigma a_\sigma \vec{N}_\sigma(\vec{r}) + \frac{Z}{j}\sum_\tau b_\tau \vec{M}_\tau(\vec{r}) \tag{23}$$

$$\vec{H}(\vec{r}) = \frac{j}{Z}\sum_\sigma a_\sigma \vec{M}_\sigma(\vec{r}) + \sum_\tau b_\tau \vec{N}_\tau(\vec{r}). \tag{24}$$

$Z = \sqrt{\mu/\epsilon}$ denotes the intrinsic impedance of the medium. The a_σ are the multipole amplitudes of the TM modes and the b_τ are the multipole amplitudes of the TE modes.

IV. SCATTERING OF ELECTROMAGNETIC WAVES BY A PERFECTLY CONDUCTING SEMI-INFINITE ELLIPTIC CONE

Now we want to obtain the solution of Maxwell's equations containing an electric current density $\vec{J}$ leading to the nonhomogeneous vector differential equation for the electric field intensity

$$\vec{\nabla} \times \vec{\nabla} \times \vec{E} - \kappa^2 \vec{E} = -j\omega\mu\vec{J}. \tag{25}$$

The electric field intensity can be calculated by the integral transformation

$$\vec{E}(\vec{r}) = \iiint_V \tilde{\Gamma}(\vec{r},\vec{r}')\vec{J}(\vec{r}')\,dv' \tag{26}$$

if the Green's dyadic function $\tilde{\Gamma}(\vec{r},\vec{r}')$ satisfies the differential equation

$$\vec{\nabla} \times \vec{\nabla} \times \tilde{\Gamma}(\vec{r},\vec{r}') - \kappa^2\tilde{\Gamma}(\vec{r},\vec{r}') = -j\omega\mu\tilde{I}\delta(\vec{r}-\vec{r}') \tag{27}$$

where $\tilde{I}$ is the unit dyadic and δ denotes Dirac's δ function. A suitable representation for the Green's dyadic in the source-free region is

$$\tilde{\Gamma}(\vec{r},\vec{r}') = -\kappa\omega\mu\left\{\sum_\sigma \frac{\vec{N}_\sigma^I(\vec{r})\vec{N}_\sigma^{II}(\vec{r}')}{\sigma(\sigma+1)} + \sum_\tau \frac{\vec{M}_\tau^I(\vec{r})\vec{M}_\tau^{II}(\vec{r}')}{\tau(\tau+1)}\right\} \quad |\vec{r}| < |\vec{r}'| \tag{28}$$

where dyadic products of the vector spherical multipole functions $\vec{N}_\sigma$ and $\vec{M}_\tau$ occur. The upper index I and II indicates the use of spherical Bessel functions and spherical Hankel functions of the second kind, respectively. Then the condition of finite energy for all values of r including $r = 0$ and Sommerfeld's radiation condition for r' tending to ∞ are automatically satisfied. A Hertz dipole source located at $\vec{r}_0$,

polarized in direction of the unit vector $\hat{a}$, and with a current moment $I\Delta l$ is described by

$$\vec{J}(\vec{r}') = I\Delta l\delta(\vec{r}' - \vec{r}_0)\hat{a} \tag{29}$$

and generates the electric field intensity

$$\vec{E}(\vec{r}) = -E_0\left\{\sum_\sigma \underbrace{\frac{\vec{N}_\sigma^{II}(\vec{r}_0)\cdot\hat{a}}{\sigma(\sigma+1)}}_{\sim a_\sigma}\vec{N}_\sigma^{I}(\vec{r}) + \sum_\tau \underbrace{\frac{\vec{M}_\tau^{II}(\vec{r}_0)\cdot\hat{a}}{\tau(\tau+1)}}_{\sim b_\tau}\vec{M}_\tau^{I}(\vec{r})\right\} \tag{30}$$

where $E_0 = I\Delta l\kappa\omega\mu$. By comparison with (23), we obtain the corresponding multipole amplitudes a_σ and b_τ. Moving the dipole toward infinity in the direction (ϑ_0, φ_0) and considering a "source-strength factor," we obtain the solution of the boundary value problem for a plane electromagnetic wave with unit amplitude, polarized in $\hat{a}$ direction, incident from direction (ϑ_0, φ_0) upon the semi-infinite elliptic cone

$$\vec{E}(\vec{r}) = \sum_\sigma \alpha_\sigma \vec{N}_\sigma^{I}(\vec{r}) + \frac{Z}{j}\sum_\tau \beta_\tau \vec{M}_\tau^{I}(\vec{r}) \tag{31}$$

$$\vec{H}(\vec{r}) = \frac{j}{Z}\sum_\sigma \alpha_\sigma \vec{M}_\sigma^{I}(\vec{r}) + \sum_\tau \beta_\tau \vec{N}_\tau^{I}(\vec{r}) \tag{32}$$

with the multipole amplitudes α_σ and β_τ

$$\alpha_\sigma = 4\pi E_0 \frac{e^{j(\sigma+1)\pi/2}}{\sigma(\sigma+1)}[\vec{n}_\sigma(\vartheta,\varphi)\cdot\hat{a}]_{\substack{\vartheta=\vartheta_0\\ \varphi=\varphi_0}} \tag{33}$$

$$\beta_\tau = 4\pi\frac{E_0}{Z}\,\frac{e^{j(\tau+1)\pi/2}}{\tau(\tau+1)}[\vec{m}_\tau(\vartheta,\varphi)\cdot\hat{a}]_{\substack{\vartheta=\vartheta_0\\ \varphi=\varphi_0}}. \tag{34}$$

By replacing the spherical Bessel functions by their asymptotic representations

$$j_\nu(\kappa r) \approx \frac{1}{2}\left(\frac{e^{j\kappa r}}{\kappa r}e^{-j(\nu+1)\pi/2} + \frac{e^{-j\kappa r}}{\kappa r}e^{j(\nu+1)\pi/2}\right) \qquad \kappa r \gg \nu \tag{35}$$

we obtain the far field as sums of inwardly and outwardly traveling waves

$$\begin{aligned}\vec{E}_\infty(\vec{r}) &= -2\pi j E_0\frac{e^{j\kappa r}}{\kappa r}\\ &\quad\cdot\left(\sum_\sigma \frac{1}{\sigma(\sigma+1)}[\vec{n}_\sigma(\vartheta,\varphi)\cdot\hat{a}]_{\substack{\vartheta=\vartheta_0\\ \varphi=\varphi_0}}\cdot\vec{n}_\sigma(\vartheta,\varphi) + \sum_\tau \frac{1}{\tau(\tau+1)}[\vec{m}_\tau(\vartheta,\varphi)\cdot\hat{a}]_{\substack{\vartheta=\vartheta_0\\ \varphi=\varphi_0}}\cdot\vec{m}_\tau(\vartheta,\varphi)\right)\\ &\quad - 2\pi j E_0\frac{e^{-j\kappa r}}{\kappa r}\\ &\quad\cdot\left(\sum_\sigma \frac{e^{j\sigma\pi}}{\sigma(\sigma+1)}[n_\sigma(\vartheta,\varphi)\cdot\hat{a}]_{\substack{\vartheta=\vartheta_0\\ \varphi=\varphi_0}}\cdot\vec{n}_\sigma(\vartheta,\varphi) - \sum_\tau \frac{e^{j\tau\pi}}{\tau(\tau+1)}[\vec{m}_\tau(\vartheta,\varphi)\cdot\hat{a}]_{\substack{\vartheta=\vartheta_0\\ \varphi=\varphi_0}}\cdot\vec{m}_\tau(\vartheta,\varphi)\right)\\ &= \vec{E}^i(\vec{r}) + \vec{E}^s(\vec{r}).\end{aligned} \tag{36}$$

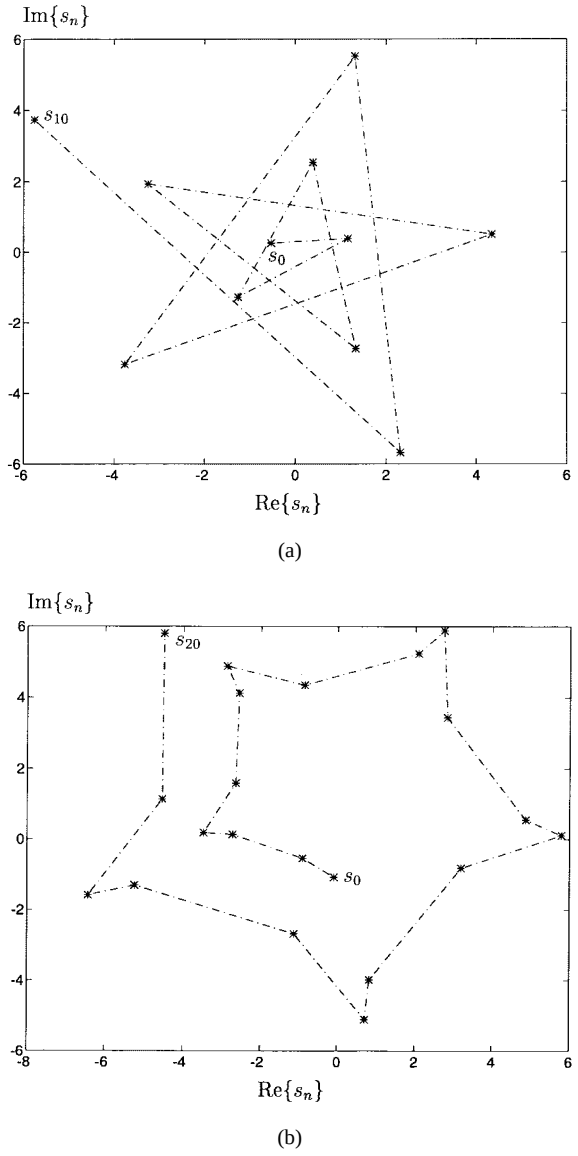

Fig. 2. Complex valued partial sums s_n of the series in (37) for a circular cone. (a) Backscattering direction $\overline{\vartheta} = 0°, \overline{\varphi} = 0°$. (b) Direction $\overline{\vartheta} = 100°, \overline{\varphi} = 0°$.

The completeness relation, applied to the complete set of normalized Lamé products $Y_\sigma(\vartheta,\varphi)$ or $Y_\tau(\vartheta,\varphi)$ allows us to show that the inwardly traveling waves represent the incident plane wave asymptotically, whereas the outwardly traveling waves represent the scattered wave. In the far field the scattered electric field intensity $\vec{E}^s(\vec{r})$ has two independent components depending on the polarization of the incident electric field intensity $\vec{E}^i(\vec{r})$

$$\begin{aligned}E_\vartheta^s &= -2\pi j E_0\frac{e^{-j\kappa r}}{\kappa r}\\ &\quad\cdot\left(\sum_\sigma \frac{e^{j\sigma\pi}}{\sigma(\sigma+1)}[\vec{n}_\sigma(\vartheta,\varphi)\cdot\hat{a}]_{\substack{\vartheta=\vartheta_0\\ \varphi=\varphi_0}}\frac{1}{s_\vartheta}\frac{\partial Y_\sigma(\vartheta,\varphi)}{\partial\vartheta} + \sum_\tau \frac{e^{j\tau\pi}}{\tau(\tau+1)}[\vec{m}_\tau(\vartheta,\varphi)\cdot\hat{a}]_{\substack{\vartheta=\vartheta_0\\ \varphi=\varphi_0}}\frac{1}{s_\varphi}\frac{\partial Y_\tau(\vartheta,\varphi)}{\partial\varphi}\right)\end{aligned} \tag{37}$$

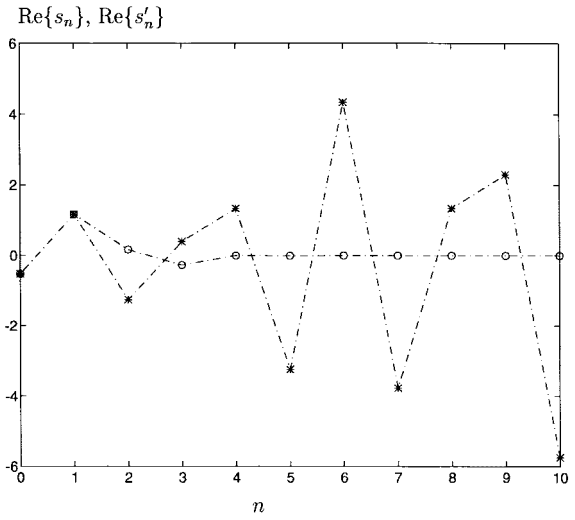

(a)

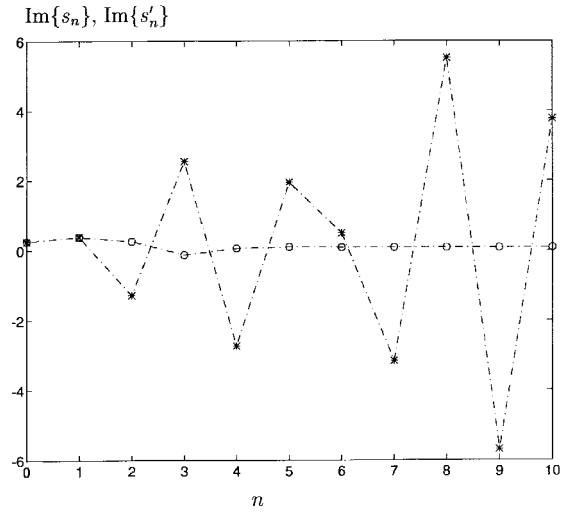

(b)

Fig. 3. (a) Real part and (b) imaginary part of the complex valued partial sums s_n $(*)$ in Fig. 2(a) and the transformed partial sums s'_n $(\circ)$ determined by (54).

$$E^s_\varphi = -2\pi j E_0 \frac{e^{-j\kappa r}}{\kappa r} \cdot \left(\sum_\sigma \frac{e^{j\sigma\pi}}{\sigma(\sigma+1)} [\vec{n}_\sigma(\vartheta,\varphi)\cdot\hat{a}]_{\substack{\vartheta=\vartheta_0\\ \varphi=\varphi_0}} \frac{1}{s_\varphi} \frac{\partial Y_\sigma(\vartheta,\varphi)}{\partial\varphi} - \sum_\tau \frac{e^{j\tau\pi}}{\tau(\tau+1)} [\vec{m}_\tau(\vartheta,\varphi)\cdot\hat{a}]_{\substack{\vartheta=\vartheta_0\\ \varphi=\varphi_0}} \frac{1}{s_\vartheta} \frac{\partial Y_\tau(\vartheta,\varphi)}{\partial\vartheta} \right). \tag{38}$$

Dependent on the direction of incidence, the polarization, and the field point these expressions may simplify because of symmetry properties of the Lamé products.

This far-field relation between the scattered field and the incident field allows us to introduce a dyadic diffraction coefficient $\tilde{D}$ according to the rules of high-frequency solutions like GTD and UTD, which state that the scattered field is an outgoing spherical wave depending only on the incident field at the tip of the scatterer and the diffraction coefficient.

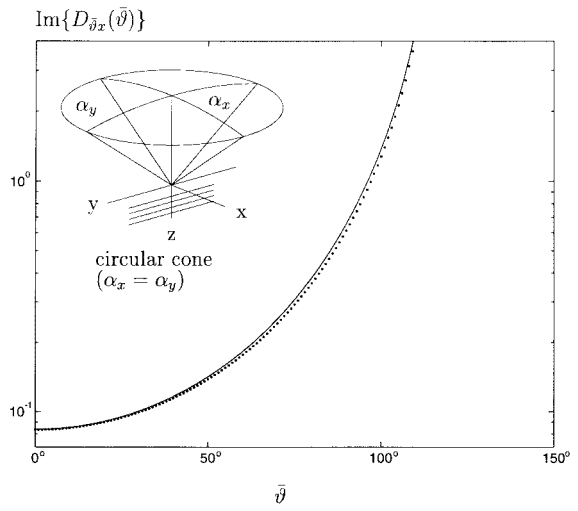

(a)

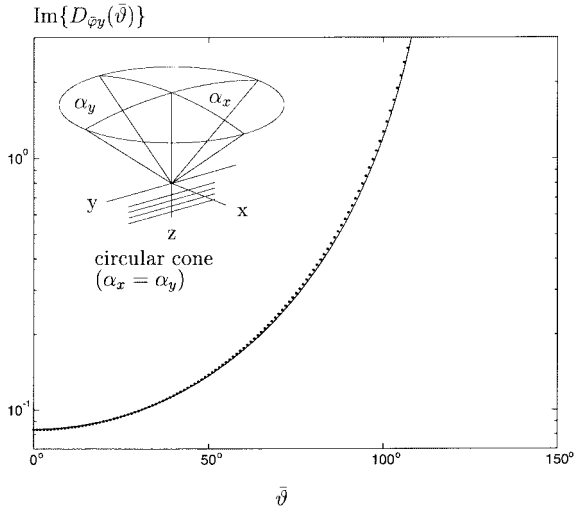

(b)

Fig. 4. Diffraction coefficients of a circular cone ($\alpha_x = \alpha_y = 30°$) in the xz plane for an axially incident plane wave ($\vartheta_0 = 0°, \varphi_0 = 0°$). The incident electric field is polarized either in x or in y direction. (a) $D_{\overline{\vartheta}x}$. (b) $D_{\overline{\varphi}y}$; ——— multipole solution. · · · PO solution by Trott *et al.* [4]. $D_{\overline{\varphi}x}$ and $D_{\overline{\vartheta}y}$ vanish in the xz plane.

Of course, we don't use spheroconal coordinates (r,ϑ,φ) and components (E_ϑ, E_φ), but usual spherical coordinates $(r,\overline{\vartheta},\overline{\varphi})$ and associated components $(E_{\overline{\vartheta}}, E_{\overline{\varphi}})$ in the following representation:

$$\vec{E}^s(\vec{r}) = \tilde{D}(\overline{\vartheta},\overline{\varphi})\vec{E}^i(0)\frac{e^{-j\kappa r}}{\kappa r} \tag{39}$$

$$\Longleftrightarrow \begin{pmatrix} E^s_{\overline{\vartheta}}(\vec{r}) \\ E^s_{\overline{\varphi}}(\vec{r}) \end{pmatrix} = \begin{pmatrix} D_{\overline{\vartheta}\overline{\vartheta}}(\overline{\vartheta},\overline{\varphi}) & D_{\overline{\vartheta}\overline{\varphi}}(\overline{\vartheta},\overline{\varphi}) \\ D_{\overline{\varphi}\overline{\vartheta}}(\overline{\vartheta},\overline{\varphi}) & D_{\overline{\varphi}\overline{\varphi}}(\overline{\vartheta},\overline{\varphi}) \end{pmatrix} \cdot \begin{pmatrix} E^i_{\overline{\vartheta}}(0) \\ E^i_{\overline{\varphi}}(0) \end{pmatrix} \frac{e^{-j\kappa r}}{\kappa r} \tag{40}$$

$$\text{with} \quad \tilde{D} = \begin{pmatrix} D_{\overline{\vartheta}\overline{\vartheta}} & D_{\overline{\vartheta}\overline{\varphi}} \\ D_{\overline{\varphi}\overline{\vartheta}} & D_{\overline{\varphi}\overline{\varphi}} \end{pmatrix}. \tag{41}$$

In the case of axial incidence we will calculate the dyadic diffraction coefficient dependent on the Cartesian components

TABLE II
NORMALIZED BISTATIC RCS σ^s/Λ^2 OF A CIRCULAR CONE ($\alpha_x = \alpha_y = 30°$) FOR AN AXIALLY INCIDENT PLANE WAVE (SEE ALSO FIG. 5 FOR A DETAILED DESCRIPTION)

	Multipole solution		Trott	Babich
$\bar{\vartheta}$	σ_x^s/Λ^2	σ_y^s/Λ^2	σ^{po}/Λ^2	σ_y^s/Λ^2
0°	0.002234	0.002234	0.002210	—
7.5°	0.002285	0.002281	0.002258	0.002282
15°	0.002444	0.002443	0.002409	0.002430
22.5°	0.002738	0.002700	0.002686	0.002700
30°	0.003218	0.003137	0.003136	0.003137
37.5°	0.003978	0.003824	0.003845	0.003822
45°	0.005192	0.004905	0.004969	0.004902
52.5°	0.007195	0.006658	0.006804	0.006652
60°	0.010663	0.009635	0.009947	0.009624
67.5°	0.017079	0.015023	0.015691	0.015009
75°	0.030019	0.025640	0.027127	0.025610
82.5°	0.059266	0.049066	0.052650	0.049011
90°	0.136597	0.116456	0.119366	0.109492
97.5°	0.394544	0.308038	0.340238	0.307766
105°	1.879576	1.286367	1.434954	—

of the incident field

$$\begin{pmatrix} E_{\overline{\vartheta}}^s(\vec{r}) \\ E_{\overline{\varphi}}^s(\vec{r}) \end{pmatrix} = \begin{pmatrix} D_{\overline{\vartheta}x}(\overline{\vartheta},\overline{\varphi}) & D_{\overline{\vartheta}y}(\overline{\vartheta},\overline{\varphi}) \\ D_{\overline{\varphi}x}(\overline{\vartheta},\overline{\varphi}) & D_{\overline{\varphi}y}(\overline{\vartheta},\overline{\varphi}) \end{pmatrix} \begin{pmatrix} E_x^i(0) \\ E_y^i(0) \end{pmatrix} \frac{e^{-j\kappa r}}{\kappa r}. \tag{42}$$

The representations in (39) and (42) allow us to calculate bistatic RCS for axial incidence of the plane wave. If the electric field of the axially incident plane wave is polarized in the x direction we define

$$\sigma_x^s(\overline{\vartheta},\overline{\varphi}) = \lim_{r\to\infty} 4\pi r^2 \left| \frac{\vec{E}^s(\vec{r})}{E_x^i(0)} \right|^2. \tag{43}$$

If the electric field of the axially incident plane wave is polarized in the y direction we define

$$\sigma_y^s(\overline{\vartheta},\overline{\varphi}) = \lim_{r\to\infty} 4\pi r^2 \left| \frac{\vec{E}^s(\vec{r})}{E_y^i(0)} \right|^2. \tag{44}$$

But it is impossible to obtain the limits of the sums in (37) and (38) by simply adding up the terms of the series. Fig. 2 shows the complex valued partial sums s_n of $E_{\overline{\vartheta}}^s$ in case of a circular cone ($\alpha_x = \alpha_y = 30°$) and x polarization of the incident electric field intensity in the backscattering direction 1)$\overline{\vartheta} = 0°$ and for 2) $\overline{\vartheta} = 100°$ in the xz plane. Therefore, in order to obtain the limits sequence transformations are necessary.

V. SEQUENCE TRANSFORMATIONS

Let us consider an infinite series

$$\sum_{l=0}^{\infty} a_l = a_0 + a_1 + a_2 + \cdots. \tag{45}$$

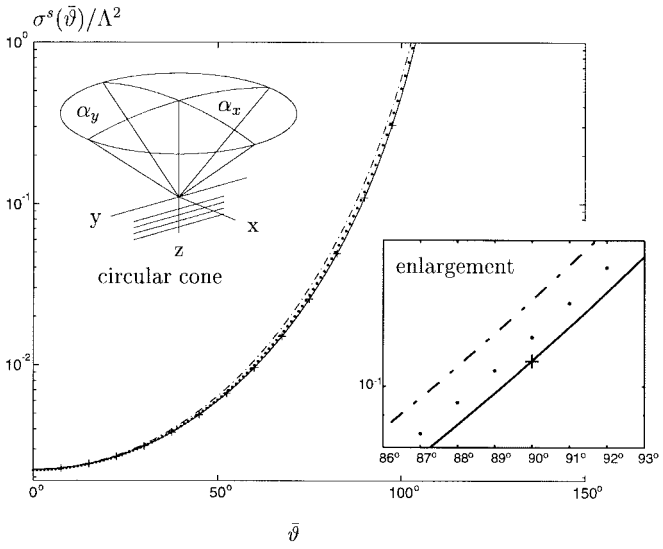

Fig. 5. Normalized bistatic RCS σ^s/Λ^2 of a circular cone ($\alpha_x = \alpha_y = 30°$) for an axially incident plane wave ($\vartheta_0 = \varphi_0 = 0$). The incident electric field is polarized either in x or y direction. The RCS are evaluated in the xz plane. ——— multipole solution σ_y^s/Λ^2 – · – ·; multipole solution $\sigma_x^s/\Lambda^2 + +\sigma_y^s/\Lambda^2$ calculated by Babich *et al.* [1]; · · · σ^{po}/Λ^2 PO-based solution (Trott [3], [4]).

The partial sums for $n+1$ terms of this series shall be denoted by s_n

$$s_n = a_0 + a_1 + a_2 + \cdots + a_n = \sum_{l=0}^{n} a_l, \qquad n = 0;1;2;\cdots. \tag{46}$$

If the sequence of the partial sums $\{s_n\}$ is converging toward a limit s

$$\lim_{n\to\infty} s_n = s \tag{47}$$

this value is the sum of the infinite series. If the sequence of the partial sums $\{s_n\}$ is not converging or very slowly converging, a transformation T can be applied to the sequence of partial sums $\{s_n\}$ in order to obtain a better converging sequence $\{s_n'\}$

$$T\{s_n\} = \{s_n'\}. \tag{48}$$

An efficient technique for calculating the sum of infinite series with poor convergence is the nonlinear Shanks transformation [13]–[16].

The kth order Shanks transformation $e_k(s_n)$ is defined in the following form:

$$e_k(s_n) = \frac{\begin{vmatrix} s_n & \cdots & s_{n+k} \\ \Delta s_n & \cdots & \Delta s_{n+k} \\ \vdots & \ddots & \vdots \\ \Delta s_{n+k-1} & \cdots & \Delta s_{n+2k-1} \end{vmatrix}}{\begin{vmatrix} 1 & \cdots & 1 \\ \Delta s_n & \cdots & \Delta s_{n+k} \\ \vdots & \ddots & \vdots \\ \Delta s_{n+k-1} & \cdots & \Delta s_{n+2k-1} \end{vmatrix}} \tag{49}$$

where the s_n are defined in (46) and $\Delta s_n = s_{n+1} - s_n$. The values $e_k(s_n)$ can be arranged in the (n,k) plane. As the

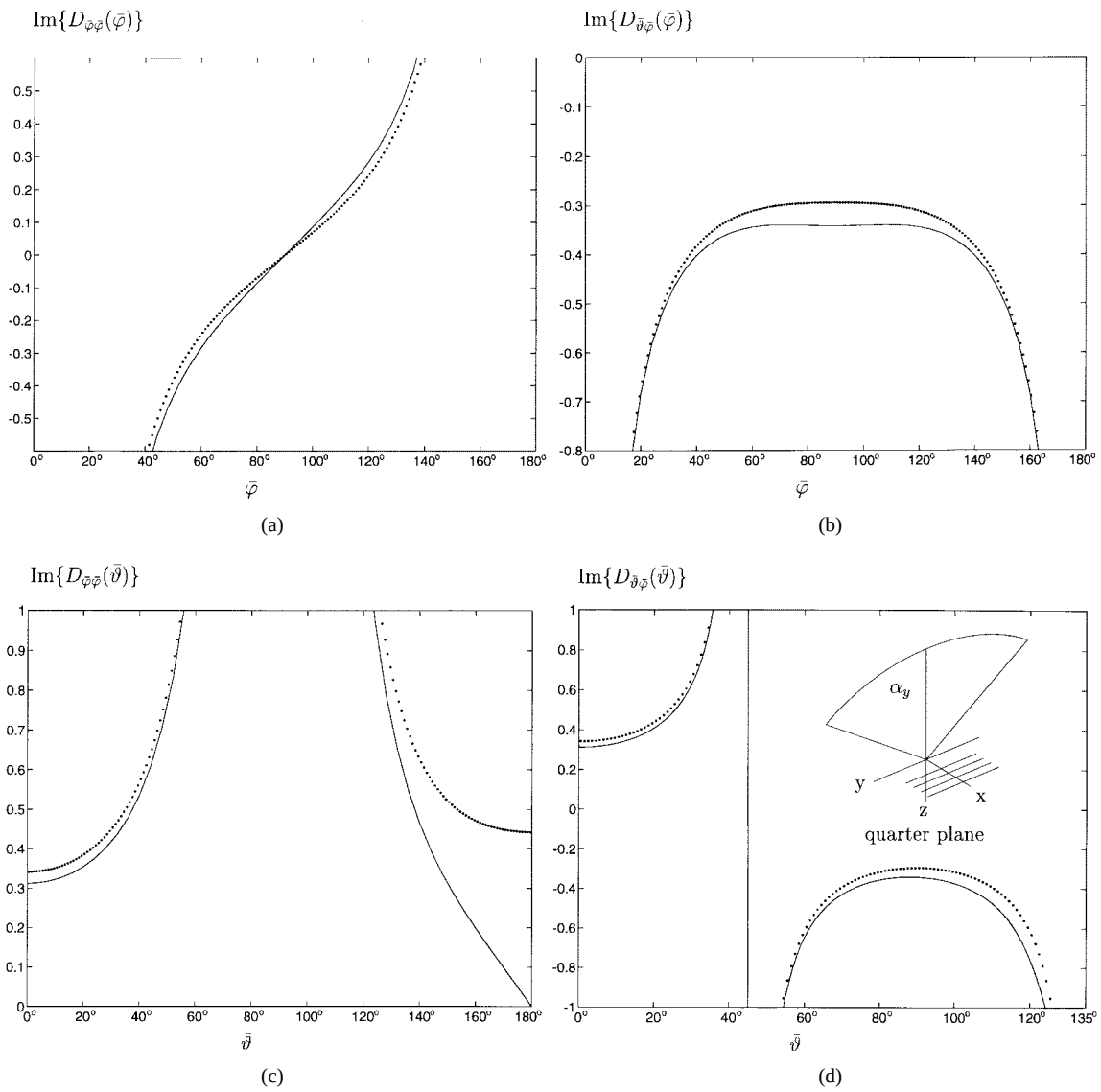

Fig. 6. Diffraction coefficients of a quarter plane ($\alpha_x = 0°, \alpha_y = 45°$) for plane wave incidence perpendicular to the plane of the sector ($\vartheta_0 = 90°, \varphi_0 = 0°$). The incident electric field is polarized in y direction, i.e. $\overline{\varphi}$-direction in this case. (a) $D_{\overline{\varphi}\overline{\varphi}}(\overline{\varphi})$ in the xy plane. (b) $D_{\overline{\vartheta}\overline{\varphi}}(\overline{\varphi})$ in the xy plane. (c) $D_{\overline{\varphi}\overline{\varphi}}(\overline{\vartheta})$ in the yz plane. (d) $D_{\overline{\vartheta}\overline{\varphi}}(\overline{\vartheta})$ in the xz plane: ____ multipole solution; · · · UTD solution by Hill [2]. $D_{\overline{\vartheta}\overline{\varphi}}$ in the xz plane and $D_{\overline{\varphi}\overline{\varphi}}$ in the yz plane vanish.

evaluation of the determinants is time consuming we apply Wynn's ϵ algorithm

$$\epsilon_{-1}^{(n)} = 0, \quad \epsilon_0^{(n)} = s_n$$
$$\epsilon_{k+1}^{(n)} = \epsilon_{k-1}^{(n+1)} + \frac{1}{\epsilon_k^{(n+1)} - \epsilon_k^{(n)}}, \qquad k, n = 0; 1; 2; \cdots \tag{50}$$

where n is the index of the partial sums and k is the order of the transformation. It can be shown that the elements with even order $2k$ yield the elements $e_k(s_n)$ of the Shanks transformation and that the elements with odd order $2k+1$ of this recursive algorithm yield only intermediate values

$$\epsilon_{2k}^{(n)} = e_k(s_n) \tag{51}$$
$$\epsilon_{2k+1}^{(n)} = \frac{1}{e_k(\Delta s_n)}. \tag{52}$$

Let us assume that only the finite sequence $(s_0, s_1, s_2, \cdots, s_n)$, i.e., $(\epsilon_0^{(0)}, \epsilon_0^{(1)}, \epsilon_0^{(2)}, \cdots, \epsilon_0^{(n)})$, of $n+1$ partial sums of the infinite series in (45) is known. According to the calculation rule in (50), we are only able to determine the following terms which can be arranged in the (n, k) plane

$$\begin{array}{ccccccccc}
\epsilon_{-1}^{(0)} & [\epsilon_0^{(0)}] & \epsilon_1^{(0)} & [\epsilon_2^{(0)}] & \epsilon_3^{(0)} & \cdots & \epsilon_{n-1}^{(0)} & \epsilon_n^{(0)} \\
\epsilon_{-1}^{(1)} & [\epsilon_0^{(1)}] & \epsilon_1^{(1)} & [\epsilon_2^{(1)}] & \epsilon_3^{(1)} & \cdots & \epsilon_{n-1}^{(1)} & \\
\vdots & \vdots & \vdots & \vdots & \vdots & & & \\
\epsilon_{-1}^{(n-2)} & \epsilon_0^{(n-2)} & \epsilon_1^{(n-2)} & \epsilon_2^{(n-2)} & & & & \\
\epsilon_{-1}^{(n-1)} & \epsilon_0^{(n-1)} & \epsilon_1^{(n-1)} & & & & & \\
\epsilon_{-1}^{(n)} & \epsilon_0^{(n)}. & & & & & &
\end{array} \tag{53}$$

As mentioned above, the elements with even order $2k$ yield the elements $e_k(s_n)$ of the Shanks transformation. Therefore,

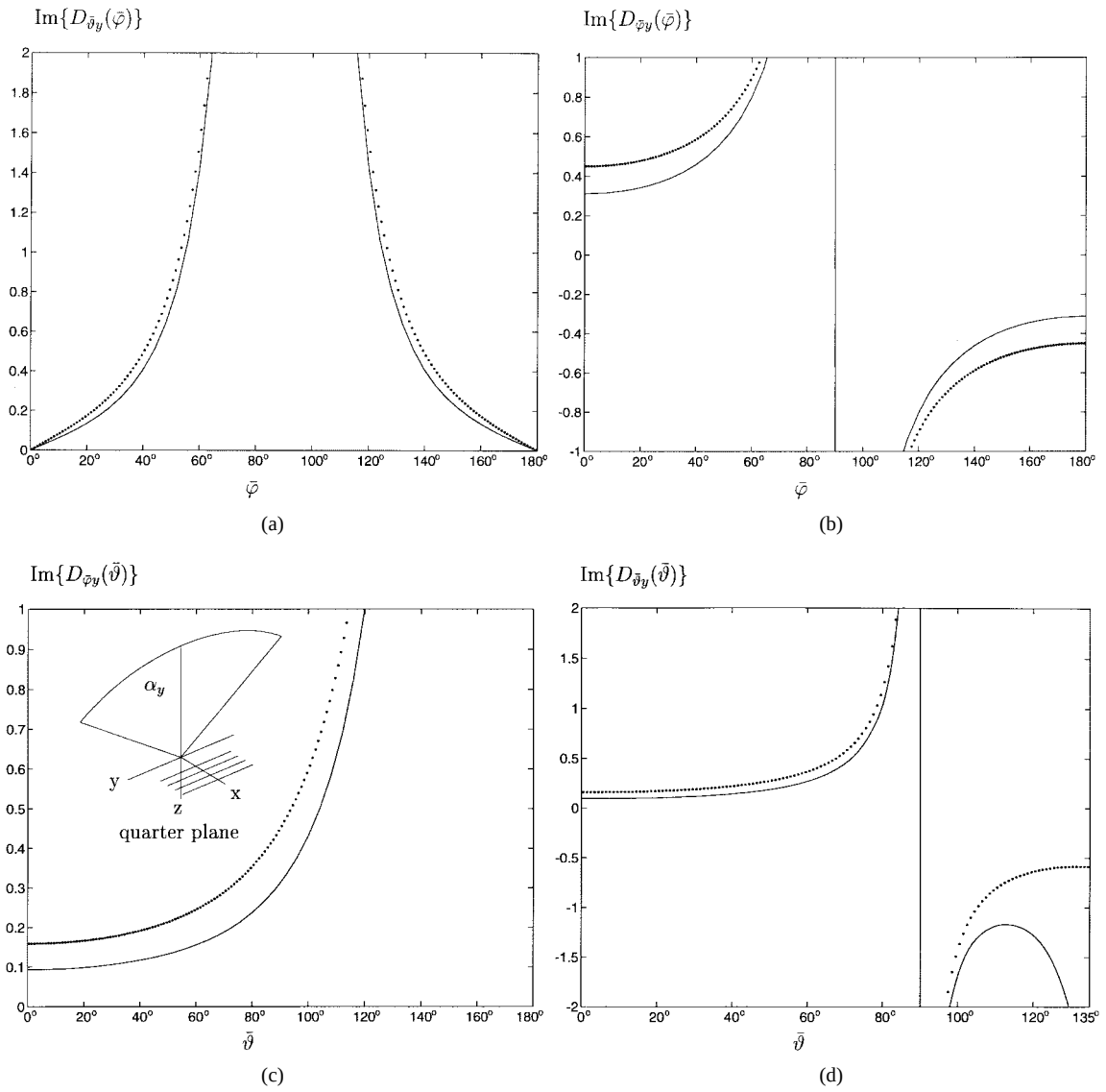

Fig. 7. Diffraction coefficients of a quarter plane ($\alpha_x = 0°, \alpha_y = 45°$) for an axially incident plane wave ($\vartheta_0 = 0°, \varphi_0 = 0°$). The incident electric field is polarized in y direction. (a) $D_{\overline{\vartheta}y}(\overline{\varphi})$ in the xy plane. (b) $D_{\overline{\varphi}y}(\overline{\varphi})$ in the xy plane. (c) $D_{\overline{\varphi}y}(\overline{\vartheta})$ in the yz plane. (d) $D_{\overline{\vartheta}y}(\overline{\vartheta})$ in the xz plane —— multipole solution; · · · UTD solution by Hill [2]. $D_{\overline{\varphi}y}$ in the xz plane and $D_{\overline{\vartheta}y}$ in the yz plane vanish.

we choose the terms in brackets to build up a new sequence

$$\{s'_n\} = (\epsilon_0^{(0)}, \epsilon_0^{(1)}, \epsilon_2^{(0)}, \epsilon_2^{(1)}, \epsilon_4^{(0)}, \cdots). \tag{54}$$

The last term will be $\epsilon_n^{(0)}$ if n is even or $\epsilon_{n-1}^{(1)}$ if n is odd. In the cases under consideration the transformed sequence $\{s'_n\}$ in (54) converges toward the same limit s as the sequence $\{s_n\}$

$$\lim_{n\to\infty} s'_n = \lim_{n\to\infty} s_n = s \tag{55}$$

if $\{s_n\}$ is a convergent sequence. Even if a sequence $\{s_n\}$ is not converging at all (like the ones in Fig. 2) the transformed sequence converges in many cases. We consider for example the complex valued sequence $\{s_n\}$ in Fig. 2(a). Although the sequence is not convergent, the transformed sequence $\{s'_n\}$ converges quickly toward a limit, which is obviously a type of mean value (Fig. 3).

The number of terms needed to obtain the limits of the series depends on the geometry considered. For all results presented in this paper a maximum number of 100 series terms was sufficient to obtain convergence. Convergence was assumed if three consecutive terms of the transformed series differed in less than the required relative accuracy of 10^{-8}.

VI. Numerical Results

We will begin with the calculation of the diffraction coefficients and the bistatic RCS for a semi-infinite perfectly conducting circular cone ($\alpha_x = \alpha_y = 30°$) in the case of an axially incident plane wave ($\vartheta_0 = 0°, \varphi_0 = 0°$). In Fig. 4, we compare the numerical results for the diffraction coefficients of the circular cone obtained with the aid of the rigorous multipole solution and the numerical results obtained with the aid of the PO-based solutions derived by Trott *et al.* [3], [4]. We assumed that the observation point is on the shadow side of the reflection boundary, i.e.,

$$0 \le \overline{\vartheta} \le \overline{\vartheta}_{RB} = \pi - 2\alpha_x \tag{56}$$

where $\overline{\vartheta}_{RB}$ denotes the direction of the reflection shadow boundary.

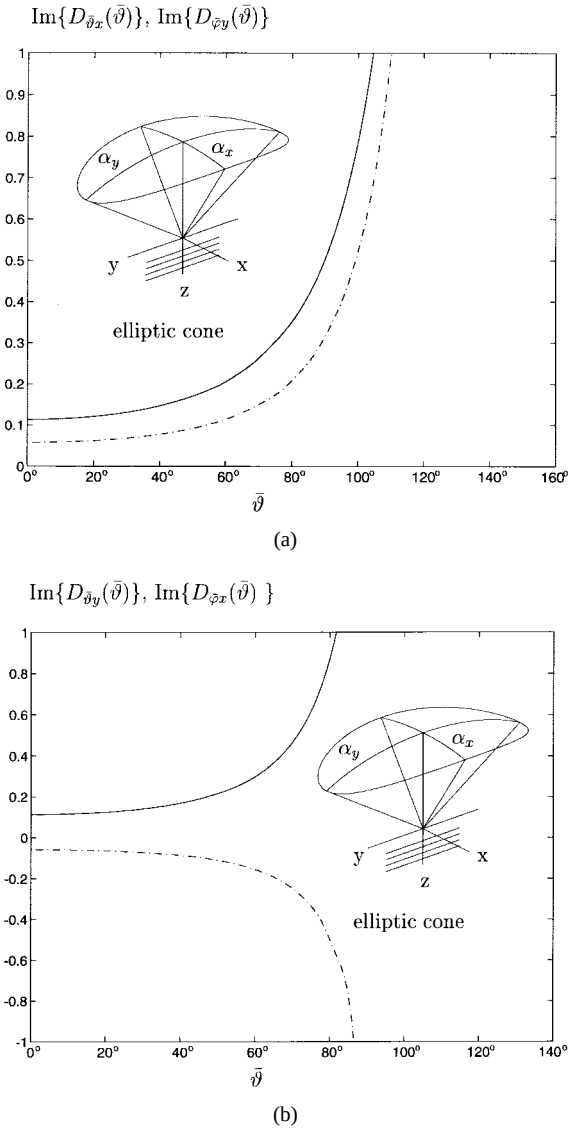

Fig. 8. Diffraction coefficients of an elliptic cone ($\alpha_x = 20°, \alpha_y = 40°$) for an axially incident plane wave ($\vartheta_0 = 0°, \varphi_0 = 0°$) determined with the aid of the multipole solution. The incident electric field is polarized either in x or y direction. The diffraction coefficients are evaluated in the xz plane and in the yz plane. (a) xz plane: $- \cdot - \cdot - D_{\overline{\vartheta}x}(\overline{\vartheta})$ ——— $D_{\overline{\varphi}y}(\overline{\vartheta})$. (b) yz plane: $- \;\; - \;\; - \;\; - D_{\overline{\varphi}x}(\overline{\vartheta})$ ——— $D_{\overline{\vartheta}y}(\overline{\vartheta})$. $D_{\overline{\varphi}x}$ and $D_{\overline{\vartheta}y}$ vanish in the xz plane. $D_{\overline{\vartheta}x}$ and $D_{\overline{\varphi}y}$ vanish in the yz plane.

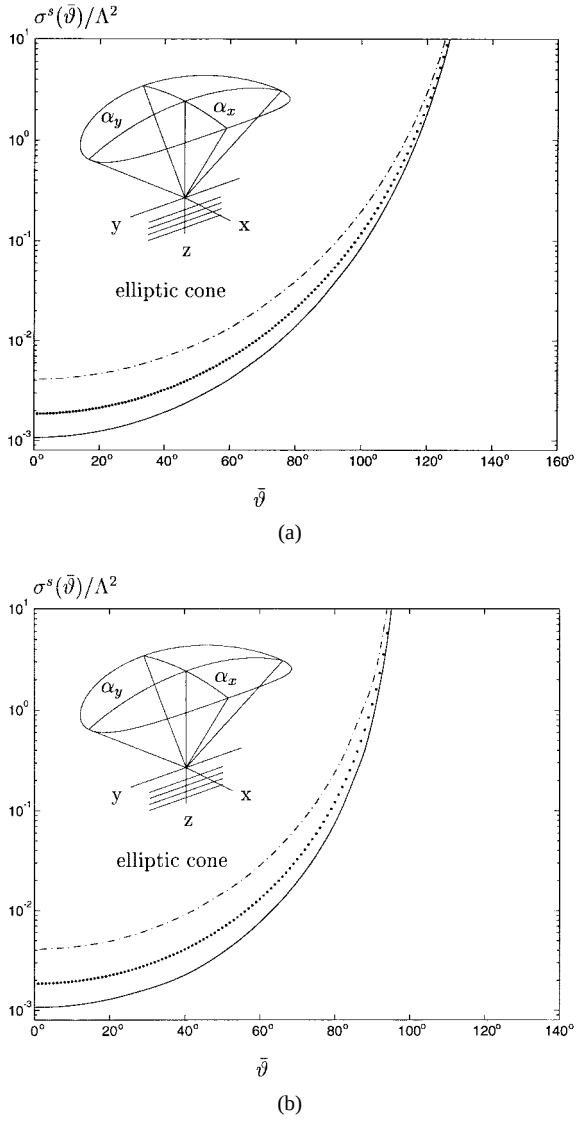

Fig. 9. Normalized bistatic RCS σ^s/Λ^2 of an elliptic cone ($\alpha_x = 20°, \alpha_y = 40°$) for an axially incident plane wave ($\vartheta_0 = 0°, \varphi_0 = 0°$). The incident electric field is polarized either in x or y direction. The RCS are evaluated in the xz plane and in the yz plane. (a) xz plane: ——— multipole solution σ_x^s/Λ^2; $- \cdot - \cdot -$ multipole solution σ_y^s/Λ^2; $\cdot \;\; \cdot \;\; \cdot \; \sigma^{po}/\Lambda^2$ PO-based solution by Blume and Kahl [5]. (b) yz plane: ——— multipole solution; σ_x^s/Λ^2 $- \cdot - \cdot -$ multipole solution; $\sigma_y^s/\Lambda^2 \cdot \;\; \cdot \;\; \cdot \; \sigma^{po}/\Lambda^2$ PO-based solution by Blume and Kahl [5].

Generally, the diffraction coefficient is a complex quantity. But at least for plane wave incidence in x, y, and z direction the real part vanishes identically for all values of the variable $\overline{\vartheta}$ or $\overline{\varphi}$ in the main planes of the elliptic cone: the xz, yz, and the xy plane. Therefore, we depicted only the imaginary parts of the diffraction coefficients in Fig. 5 and (in the following) Figs. 6–8. In Table II and Fig. 5, numerical values for the bistatic RCS σ_x^s/Λ^2 and σ_y^s/Λ^2 of a circular cone, calculated with the aid of the rigorous multipole solution in the xz plane, are compared with the available data obtained by Babich *et al.* [1] and with data calculated with the PO-based solution derived by Trott *et al.* [3], [4].

Subsequently, we will calculate the diffraction coefficients of the quarter plane ($\alpha_x = 0°, \alpha_y = 45°$) for a plane wave with incidence perpendicular to the plane of the sector ($\vartheta_0 = 90°, \varphi_0 = 0°$) (Fig. 6) and for an axially incident plane wave (Fig. 7). We compare the numerical results obtained with the aid of the rigorous multipole solution and the numerical results obtained with the aid of the UTD solution derived by Hill [2]. The UTD solution was evaluated in the far zone for purpose of comparison with the far-zone field of the multipole solution. Note that no scattered field is produced by the sector for axial incidence of the plane wave, if the electric field is polarized in x direction, i.e., perpendicular to the sector plane.

Finally, we will calculate numerically—with the aid of the multipole solution—the diffraction coefficients of an elliptic cone ($\alpha_x = 20°, \alpha_y = 40°$) for an axially incident plane wave. The incident electric field is polarized either in x or y direction. The diffraction coefficients are evaluated in the xz plane and the yz plane. The results are depicted in Fig. 8.

In Fig. 9, numerical values for the bistatic RCS σ_x^s/Λ^2 and σ_y^s/Λ^2 of this elliptic cone (using the multipole solution) are compared with data calculated with the PO-based solution derived by Blume and Kahl [5].

Our results for the RCS σ_y^s/Λ^2 of a circular cone—evaluated in the xz plane in the case of an axially incident plane wave whose electric field is polarized in the y direction—are in very good agreement with those ones calculated by Babich *et al.* [1, (Fig. 5 and Table II)]. But they did not evaluate the RCS σ_x^s/Λ^2 in the xz plane for x polarization of the axially incident plane wave. The RCS are slightly polarization dependent, which the PO-based approximation σ^{po}/Λ^2 derived by Trott *et al.*, does not take into account. Only two components of the dyadic diffraction coefficient of a circular cone occur in the xz plane. The other two components vanish identically. The PO-based approximation of the diffraction coefficients is in rather good agreement with the results obtained by evaluating numerically the rigorous multipole solution (Fig. 4).

Analogous results are obtained in the yz plane on behalf of the circular structure of the cone. Note that a reflection shadow boundary $\overline{\vartheta}_{RB}$ arises from the fact that the incident plane wave is reflected at the surface of the circular cone. For axial incidence of the plane wave this reflection boundary $\overline{\vartheta}_{RB}$ can be determined with the aid of the law of reflection: $\overline{\vartheta}_{RB} = \pi - 2\alpha_x$.

The comparison of the dyadic diffraction coefficients for a quarter plane evaluated with the aid of the multipole solution and evaluated with the aid of the UTD solution derived by Hill [2] shows sufficient agreement for vertical incidence if the field point and the source point of the scattered field are far away from each other (Fig. 6). If they coincide—this happens for example in the xz plane for $\overline{\vartheta} = 180°$ [Fig. 6(c)]—the UTD solution fails. The comparison for axial incidence (grazing incidence) in Fig. 7 additionally shows a slight difference near the backscattering direction both in the xz plane and yz plane. But axial incidence is also the worst case where a UTD solution can be used. Because of wedge diffraction phenomena at the two edges forming the quarter plane, two Keller cones occur where the diffraction coefficient tends to infinity, e.g., for axial incidence we pass through one of them in the yz plane at $\overline{\vartheta} = 90°$ [Fig. 7(d)]. The reason for the observed discrepancies is that the multipole solution does satisfy the boundary conditions whereas the UTD solution does not. Note that with the knowledge of the diffraction coefficients the RCS σ_y^s/Λ^2 can also easily be calculated.

In the case of scattering by an elliptic cone, the polarization-independent PO-based solution by Blume and Kahl [5] for the RCS of this object is only an approximation that lies between the exact data for the two polarizations (Fig. 9). Similar to the circular cone a reflection boundary occurs at elliptic cones. In the xz plane we meet this reflection boundary at $\overline{\vartheta}_{RB} = \pi - 2\alpha_x$; in the yz plane we meet this reflection boundary at $\overline{\vartheta}_{RB} = \pi - 2\alpha_y$ (Fig. 8).

VII. Conclusion

In this work, the electromagnetic wave scattering by a perfectly conducting semi-infinite elliptic cone has been treated. The rigorous solutions of this boundary value problem in the form of modal series expansions are of poor convergence. The application of the Shanks transformation directly enables us to determine dyadic diffraction coefficients and bistatic RCS of an elliptic cone, a circular cone, and a quarter plane. The results obtained are in good agreement with some published calculations performed with the aid of quite different methods.

References

[1] V. M. Babich, V. P. Smyshlyaev, D. B. Dementiev, and B. A. Samokish, "Numerical calculation of the diffraction coefficients for an arbitrary shaped perfectly conducting cone," *IEEE Trans. Antennas Propagat.*, vol. 44, pp. 740–747, May 1996.

[2] K. C. Hill, "A UTD solution to the EM scattering by the vertex of a perfectly conducting plane angular sector," Ph.D. dissertation, Ohio State Univ., Columbus, OH, 1990.

[3] K. D. Trott, "A high frequency analysis of electromagnetic plane wave scattering by a fully illuminated perfectly conducting semi-infinite cone," Ph.D. dissertation, Ohio State Univ., Columbus, OH, 1986.

[4] K. D. Trott, P. H. Pathak, and F. A. Molinet, "A UTD type analysis of the plane wave scattering by a fully illuminated perfectly conducting cone," *IEEE Trans. Antennas Propagat.*, vol. 38, pp. 1150–1160, Aug. 1990.

[5] S. Blume and G. Kahl, "The physical optics radar cross section of an elliptic cone," *IEEE Trans. Antennas Propagat.*, vol. 35, pp. 457–460, Apr. 1987.

[6] S. Blume, "Spherical multipole analysis of electromagnetic and acoustic scattering by a semi-infinite elliptic cone," *IEEE Antennas Propagat. Mag.*, vol. 38, no. 2, pp. 33–44, Apr. 1996.

[7] S. Blume, L. Klinkenbusch, and U. Uschkerat, "The radar cross section of the semi-infinite elliptic cone," *Wave Motion*, vol. 17, pp. 365–389, 1993.

[8] S. Blume and U. Uschkerat, "The radar cross section of the semi-infinite elliptic cone: Numerical evaluation," *Wave Motion*, vol. 22, pp. 311–324, 1995.

[9] L. Kraus and L. M. Levine, "Diffraction by an elliptic cone," *Commun. Pure Appl. Math.*, vol. XIV, pp. 49–68, 1961.

[10] J. A. Stratton, *Electromagnetic Theory*. New York: McGraw-Hill, 1941.

[11] J. K. M. Jansen, "Simple periodic and nonperiodic Lamé functions and their application in the theory of conical waveguides," Ph.D. dissertation, Eindhoven Univ. Technol., Eindhoven, The Netherlands, 1976.

[12] J. Boersma and J. K. M. Jansen, "Electromagnetic field singularities at the tip of an elliptic cone," Dept. Math. Comput. Sci., Eindhoven Univ. Technol., The Netherlands, EUT Rep. 90-WSK-01, 1990.

[13] C. Brezinski and M. Redivo Zaglia, *Extrapolation Methods, Theory and Practice*. Amsterdam, The Netherlands: North-Holland, 1991.

[14] E. J. Weniger, "Nonlinear sequence transformations for the acceleration of convergence and the summation of divergent series," *Comput. Phys. Rep.*, vol. 10, pp. 189–371, 1989.

[15] N. Kinayman and M. I. Aksun, "Comparative study of acceleration techniques for integrals and series in electromagnetic problems," *Radio Sci.*, vol. 30, no. 6, pp. 1713–1722, 1995.

[16] V. Krebs, "Sphärische Multipolentwicklung von Beugungsfeldern des elliptischen Kegels und ihre numerische Auswertung mit Hilfe von Reihentransformationen," Ph.D. dissertation, Ruhr-Universität Bochum, Germany, 1997.

Siegfried Blume was born in Wanne-Eickel, Germany. He received the Ph.D. degree and the Habilitation degrees in physics from the Philipps-University, Marburg, Germany, in 1959 and 1966, respectively.

From 1970 to 1976, he was a Professor of applied physics at the University of Marburg. Since 1976 he has been a Professor of theoretical electrical engineering at the Ruhr-University, Bochum, Germany. He is the author of a book on the theory of electromagnetic fields. His research interests include broad-band antennas, electromagnetic scattering and diffraction, electromagnetic compatiblity, and Fourier optics.

Dr. Blume is a member of the German Physical Society, VDE, and URSI.

Volker Krebs was born in Recklinghausen, Germany, on July 25, 1968. He received the Dipl. degree and the Ph.D. degree from Ruhr-University, Bochum, Germany, in 1993 and 1997, respectively.

Since 1993, he has been working at the Department of Electrical Engineering, Ruhr-University, Bochum. His research interests include diffraction theory, sequence transformation, and numerical computation in applied electromagnetics.